https://dx.doi.org/10.22161/ijaers.611.57 ISSN: 2349-6495(P) | 2456-1908(O)

A CFD Analysis of Wind Effects on Lifted Loads

Felipe Almeida Monteiro, Roger Matsumoto Moreira

Computational Fluid Dynamics Laboratory, School of Engineering, Fluminense Federal University, Brazil

Abstract*—This work presents a numerical investigation of the effects of wind blowing on lifted structures. The chosen case is an offshore oil & gas platform module lifted by a crane. The pendulum-like displacement of the lifted load is expected once wind blows on it, therefore a pendulum-like displacement is determined via a finite difference scheme whereas drag coefficients of the platform module are estimated through Computational Fluid Dynamics (CFD) via a finite volume method. Numerical results are compared to empirical data found in the literature and experiments carried out in a scaled model. Displacements of the lifted load are calculated for different gusts of wind and compared to standards commonly used by the oil & gas industry. It is confirmed that the recommended horizontal gap around the lifted structure is adequate for wind speeds of up to 20 m/s. For higher wind velocities, displacements become too large for a safe rigging and hook-up operation.*

***Keywords*—Aerodynamics, CFD, fluid-structure interaction, lifting.**

I. INTRODUCTION

The offshore oil & gas industry is continuously evolving to explore more complex resources at higher rates, reaching deeper depths, harsher environments and unconventional reservoirs. Increased complexity requires more equipment that leads to larger and heavier facilities, which become more challenging to assemble. With the world's growing energy demand [1], it is understood that such facilities will continue to be built in the years to come as oil and gas will remain a significant part of the global energy mix.

Efforts to build platforms more efficiently and safely have led to several assembly methods such as modularization [2]. It consists of separate modules built separately in different locations and integrated together onto the final unit. Despite its broad use throughout the industry, it is argued that poor module architecture increases costs due to inefficient assembly, among other issues [3]. Integration and commissioning phases' complexity have led to project schedules and cost overruns of over 100%. To minimize risks associated with construction, integration and commissioning phases, modules' dimensions have increased while their quantities have been reduced, aiming to have the least possible scope to be executed on the final unit. Nevertheless, increasing modules' dimensionsjeopardisesthe most complex step of modularization: lifting and transportation. Fig. 1 shows the lifting operation of a living quarter module of a platform, weighting just above 3000 tons.

Heavy lifting operation is a complex and dynamic problem. Beyond its own weight, which solicits structurally the lift crane and accessories (eye bolts, shackles and slings), the lifted load is subject to accelerations due to engineering and environmental factors. The lifted structure's vertical speed, added to crane's horizontal speed, added to unexpected accelerations of the crane or of the load may produce undesirable displacements. Therefore, soil stability, wave activity and wind gusts must be clearly stated in the lifting plan as conditions to execute the operation. These shall be carefully analyzed and monitored to guarantee a safe rigging operation onshore and offshore. For instance, the tragic accident of the Milwaukee Brewers Basketball Stadium, was caused by lateral wind loads acting on the lifted load and crane boom [4].

Fig.1: Rigging of a living quarter module of a platform.

This work aims to provide a CFD approach to estimate the pendulum-like displacement of lifted structures due to wind effects. CFD analysis is utilized to estimate the drag coefficient (C_D) of wind flow around the lifted platform module as it is a tool broadly used to solve industry problems [5], to model air flow in various applications[6], and to model hydrodynamic events [7].

https://dx.doi.org/10.22161/ijaers.611.57 *ISSN: 2349-6495(P) | 2456-1908(O)*

II. METHOD

A commercial CFD package, ANSYS CFX, release 15.0 is utilized to estimate drag coefficients for wind flow around the lifted load at different wind speeds. The pendulum-like displacement is then calculated via a finite difference scheme, using the CFD obtained drag coefficient as an input. The work is divided in four phases: set up a finite difference mathematical scheme that models pendulous motion, test it experimentally, obtain$C_D$for air flow around an oil & gas platform module (lifted load) through CFD and couple both analysis to obtain the load displacement.

In order to avoid running analysis not needed for the purpose of this work, a simplification was adopted, and a particularity shall be noted.Once a lifted body is set into motion by wind, a rotational and spinning movement can occur. As this work focus on potential for collision with nearby structures and people, lifted body motion is assumed to be a two-dimensional pendulous like movement. Such simplification has been previously adopted [8].

Further, modules of oil and gas platforms can be composed by various equipment of different shapes, allowing wind to flow through the module. The module utilized in this work is impermeable, there is no wind flow through its boundaries, it represents an electrical room, which is mostly enclosed by steel plates, similarly to the one shown in Fig. 1 (living quarter module).

2.1. Pendulum Mathematical Model

The mathematical model is based on the diagram shown in Fig. 2.

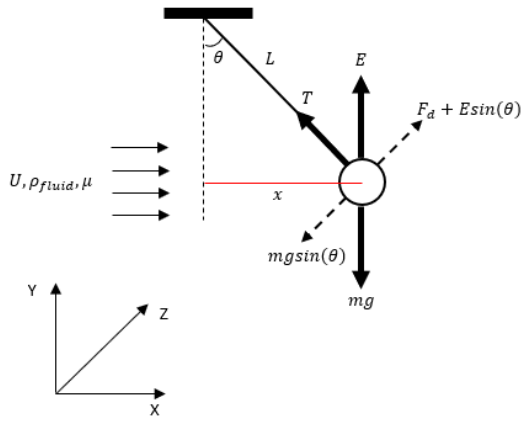

Fig.2: Pendulum model

There are three forces acting in the tangential direction: drag (F_D), weight (mg) tangential component and buoyancy (E) tangentialcomponent,where F_t represents the tangential forces, m is the pendulum mass, a_t is the tangential acceleration, L is the pendulum's cable length, T is the cable traction, x represents load's horizontal displacement from vertical position, θ is the pendulum opening angle, g is the gravity acceleration, E is the

$$\sum F_t = m\,a_t = m\,L\left(\frac{d^2\theta}{dt^2}\right) = -mg\sin(\theta) + E\sin(\theta) + F_D \quad (1)$$

boyuancy, μ fluid dinamic viscosity, $\rho_{fluid}$is the fluid density, U fluid velocity and F_D is the drag force. By applying Newton's second law:

Where:

$$F_D = \frac{C_D \rho_{fluid}\,(vel)^2 A}{2} \quad (2)$$

in which A is the body's area and vel is body's linear relative velocity to fluid, which can be written as:

$$vel = U\cos(\theta) - \omega L, \quad (3)$$

where ω is the pendulum's angular velocity.

Equation (1) can be written as:

$$\frac{d^2\theta}{dt^2} = \alpha\sin(\theta) + \beta \quad (4)$$

Where:

$$\alpha = -\frac{g}{L}\left(1 - \frac{\rho_{fluid}}{\rho_{body}}\right) \quad (5)$$

$$\beta = \pm\frac{C_D vel^2 A \rho_{fluid}}{2\,mL} \quad (6)$$

where ρ_{body} represents body's density.

In order to obtain the lateral displacement, it is needed to determine the opening angle θ at each time step. For this purpose, equation 4 is solved by means of an explicit fourth-order Runge-Kutta method, motivated by previous similar application [9] to solve a pendulum model immersed in fluid. Such method requires four auxiliary values (k_{1-8})for each solved variable. Therefore, equations for $\theta(t)$ and $\omega\,(t)$ are written as:

https://dx.doi.org/10.22161/ijaers.611.57 *ISSN: 2349-6495(P) | 2456-1908(O)*

$$\omega_{n+1} = \omega_n + \frac{1}{6}(k_1 + 2k_3 + 2k_5 + k_7) \quad (8)$$

$$\theta_{n+1} = \theta_n + \frac{1}{6}(k_2 + 2k_4 + 2k_6 + k_8) \quad (9)$$

Where:

$$k_1 = h\, f(\omega_n, \theta_n) \quad (10)$$

$$k_2 = h\, \omega_n \quad (11)$$

$$k_3 = h\, f\left(\omega_n + \frac{k_1}{2}, \theta_n + \frac{k_2}{2}\right) \quad (12)$$

$$k_4 = h\left(\omega_n + \frac{k_1}{2}\right) \quad (13)$$

$$k_5 = h\, f\left(\omega_n + \frac{k_3}{2}, \theta_n + \frac{k_4}{2}\right) \quad (14)$$

$$k_6 = h\left(\omega_n + \frac{k_3}{2}\right) \quad (15)$$

$$k_7 = h\, f(\omega_n + k_5, \theta_n + k_6) \quad (16)$$

$$k_8 = h\,(\omega_n + k_5) \quad (17)$$

where *h* is the time step.

2.2. Experimental Model

In order to test and validate the mathematical model proposed in section 2.1, a scaled model experiment was developed. The purpose with the experiment is to test whether the mathematical model can determine the same motion observed in the experiment under the same conditions.

For this analysis, the chosen geometry for the pendulum is a sphere as $C_D$for flow around it can be easily obtained by an empirical formula [10]which has adequate accuracy for Reynolds number ranging from 0 to $2x10^5$:

$$C_{Dsphere} = \frac{24}{Re} + \frac{6}{1+\sqrt{Re}} + 0{,}4 \quad (18)$$

The experiment is made using a glass reservoir partially filled with water where a metallic sphere (200mm of diameter, 1930 kg/m³ of density) hangs by a nylon cable (154mm in length) immersed in water and a digital photographic camera (Panasonic LUMIX DMC-FZ5) stands on a tripod outside of the reservoir. The sphere is placed at an initial angle (θ_0) of 33 degrees, as shown in Fig. 3 and then at *t=0+h* it is released to swing. It is considered that the sphere only moves along the θ direction. To acquire the time response of angle θ, the digital camera captures (at a rate of 60 frames per second) the motion, which is later post-processed in MatLab.

Experiment`s angle $\theta$time response, captured by the camera, is compared topendulum mathematical model`s angle θtime responseapplying the same conditions in a combined plot.

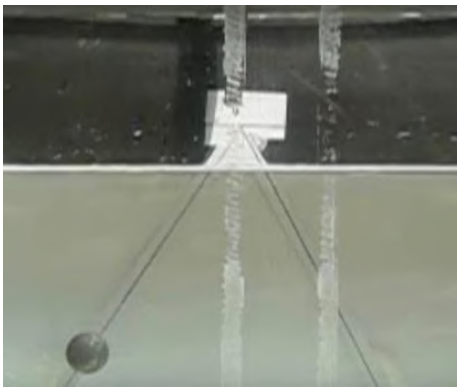

Fig.3: Sphere immersed in fluid placed at an initial angle of 33 degrees

2.3. CFD Analysis for Drag Coefficient Estimation

As presented by equation (2), the $C_D$for flow around the body is needed to estimate the drag force acting on it when subjected to air flow. To obtain C_D is a challenge that has been extensively studied by many, therefore several methods are available. This work has selected to use two of them: empirical formula and CFD analysis.

At first, a cylinder geometry is selected to test whether CFD is an adequate method to estimate C_D, motivated by the previous application with the same objective [11] and the existance ofan empirical formula that estimates the C_D for flow around a cylinder [12] with adequate accuracy for Reynolds number ranging from 10^{-4} to $2x10^5$:

$$C_{Dcylinder} = 1{,}18 + \frac{6{,}8}{Re^{0{,}89}} + \frac{1{,}96}{Re^{0{,}5}} - \frac{0{,}0004Re}{1+3{,}64^{-7Re^2}} \quad (19)$$

An unsteady compressible flow over the cylinder was modeled by means of a commercial CFD software, ANSYS. Computational grids were generated with ANSYS ICEM 16.0. Long run computations were adopted in order to guarantee that a steady-state regime was achieved. All the computations were carried out on a 64 bit, 3.40 GHz Intel Core i7-2600 processor with 16 Gb of RAM. The unsteady flow is modeled in two-dimensions i.e. in the x-y plane (see Fig. 2), with mass and momentum being conserved in the fluid domain. To determine the velocity and pressure fields, a homogeneous multiphase Eulerian fluid approach is used. Continuity and Navier-Stokes equations are given by:

$$\frac{\partial \rho}{\partial t} + \nabla \cdot (\rho \boldsymbol{u}) = 0 \quad (20)$$

$$\rho \frac{D\boldsymbol{u}}{Dt} = \nabla \cdot \boldsymbol{T} + \rho \boldsymbol{f} \quad (21)$$

ρ and μ are the fluid's density and viscosity; u = *(v,w)* is the fluid's velocity vector; $\boldsymbol{f}$ = (0,-g) is the acceleration due

https://dx.doi.org/10.22161/ijaers.611.57 *ISSN: 2349-6495(P) | 2456-1908(O)*

to gravity; $\boldsymbol{T}$ is the stress tensor of Newtonian fluids, which includes the effects of the dynamic pressure p and viscous forces. As the flow occurs in high Reynolds number, turbulence is taken into account by means of a Reynolds Averaged Navier-Stokes two-equation ($\kappa - \omega$) turbulence model based on the SST (Shear Stress Transport) formulation proposed by Menter (1994). The initial value problem is solved by the CFD package ANSYS CFX release 15.0, which makes use of the finite volume method [13].

Then, to estimate C_D for air flow around a platform module, the geometry is changed from a cylinder to the module. The chosen module for this study is an electrical room module from a floating production storage platform, weighting 1145 tonnes, enclosed by steel plates. Module's external dimensions are: 22,5 x 17,6 x 19,2m. From module`s lifting plan it is obtained that its sling length, holding it from the crane tip, is 47,19m long. Two dimensions projection is shown in Fig. 4.

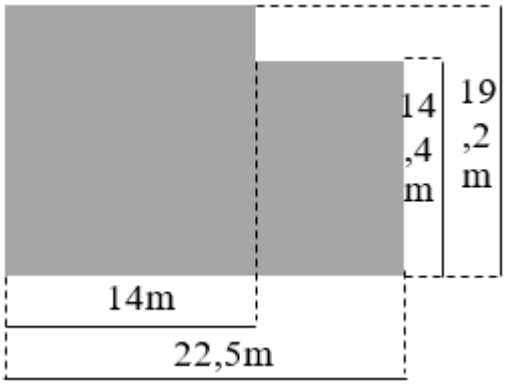

Fig.4: Module dimensions

The CFD model is an air filled domain surrounding the two dimensions module shape. Boundary conditions are such that the fluid domain at first, *t=0*, is at rest and at *t=0+h*, an uniform stream flow *U=(U,0)* is imposed to interact with the body. Four different stream velocity conditions are applied, where *U* is 10, 15, 20 and 40 *m/s*. Neumann and Dirichlet conditions (impermeable walls) are applied to all modules' surfaces, domain's lower and one side boundaries. While at domain's top and far-end boundaries atmospheric pressure is set and symmetry boundary condition is applied to other side boundary, as shown in Fig. 5.

The pressure field and shear stress are estimated and integrated across the module's area for each time step. A harmonic behavior was observed in the horizontal component of the drag force.

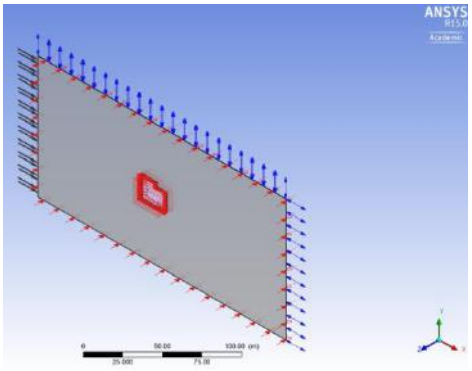

Fig. 5: CFD model set up

2.4. Wind Load and Displacement Analysis

At the final and main phase of this work, all previous phases come together for the fluid-structure interaction. The drag force induced by wind on the module is introduced into the Newton`s second law equation (1) as done in previous application [14] by coefficient for the module, obtained through CFD, is an input into equation (6) in the pendulum mathematical model. At first, *t=0,* the body is at rest and placed at $\theta = 0$,equations (3) and (4) can be written as:

$$vel = U\cos(0) \quad (22)$$

$$f(\omega, \theta) = f(0,0) = \alpha \sin(0) + \beta \quad (23)$$

at *t=0+h,* a stream flow of velocity *U=(U,0)* is introduced and maintained for 3 seconds. It is expected that the module swings in the flow direction. By using the pendulum model, module`s wind induced displacement is estimated.

From obtained angle θ time response, it is possible to calculate the module`s (lifted load) horizontal displacement through equation 24:

$$x = L\,sin(0) \quad (24)$$

L being 47,19m from module`s lifting plan.

III. RESULTS

The results are compiled in the following subsections: experimental validation, drag coefficient and wind load analysis of lifted module.

3.1. Experimental Validation

At first it is needed to confirm that the finite difference mathematical model proposed at section 2.1 can estimate the pendulous motion of a body. Fig. 6 shows the combined plot of the time response of angle θ obtained by the finite difference model (dashed line) and by the experimentally (solid line) under the same conditions.

https://dx.doi.org/10.22161/ijaers.611.57 *ISSN: 2349-6495(P) | 2456-1908(O)*

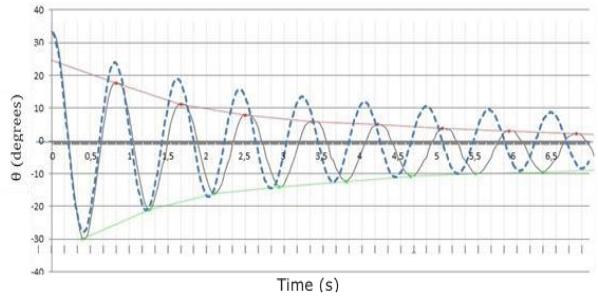

Fig 6: Angle time response

It is noticed that both models estimate maximum and minimum angle θ in the same order of magnitude. Phase shift is observed between both, which can be explained by higher drag coefficient in the experimental model due to nylon cord interaction with the fluid and sphere's surface imperfect finishing. This would also explain reduced swinging amplitude when compared to mathematical model result.

3.2. Module Drag Coefficient

CFD analysis is applied to estimate the C_D for the wind flow around the electrical room module. Prior to applying it to the module, it is verified whether CFD is an adequate method for estimatingC_D.

In Fig. 7 it is shown the C_D estimates, obtained through CFD (red squares represent a stationary regime, while blue diamonds indicate a transient one), for flow around a cylinder for Reynolds numbers up to $2\ x10^5$. The cylinder shape is chosen as a C_D x Rean empirical curve (black line)is available [15], allowing for results benchmarking.

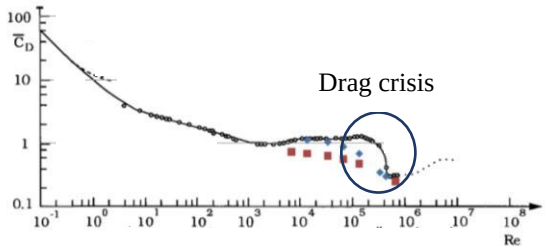

It) in the ned experimentally up to the drag crisis and even capable to capture its effects to C_D. Then, estimatedC_D (for flow around a cylinder) data by proposed CFD model (solid red line) and obtained by empirical formula, equation (19) (dotted blue line) are plotted together, shown in Fig. 8.

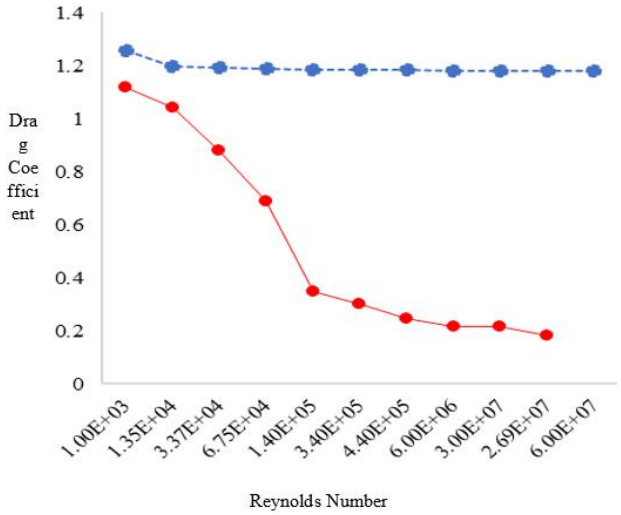

Fig. 8: Combined plot of drag coefficient estimates obtained by CFD and by empirical formula

It is noted that C_D values estimated by CFD have a more similar distribution to the empirical curve [15], shown in Fig. 7, than the values obtained by the empirical formula. Such result supports the choice of estimatingC_D values by CFD, as the modeled event occurs at Reynolds number beyond the drag crisis.

Drag coefficients estimated by CFD for flow around a module are shown in Fig. 9:

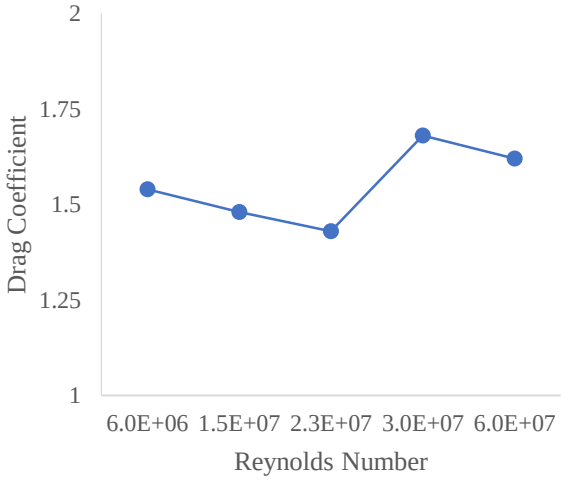

Fig.9: Module`s drag coefficients

It can be observed that estimated C_D values are of the same order of magnitude as the ones in previous application [16], approximately at 2,0 for $2x10^4 \leq Re \leq 10^6$ for a flow around a square (aspect ratio of 1). Further, it is experimentally shown [17] that the higher the shape`s aspect ratio perpendicular to the fluid flow, the lower is the C_D. This finding supports the lower estimated values (shown in Fig. 9) when compared to previous

https://dx.doi.org/10.22161/ijaers.611.57 *ISSN: 2349-6495(P) | 2456-1908(O)*

application[16] as the module has a higher aspect ratio (1,1) than the square.

3.3. Wind Load Analysis

The horizontal displacement is calculated using the C_D values estimated by CFD. Fig. 10 shows the time response of θ of the module once disturbed by wind gusts at 10, 15, 20 and 40m/s during 3 seconds.

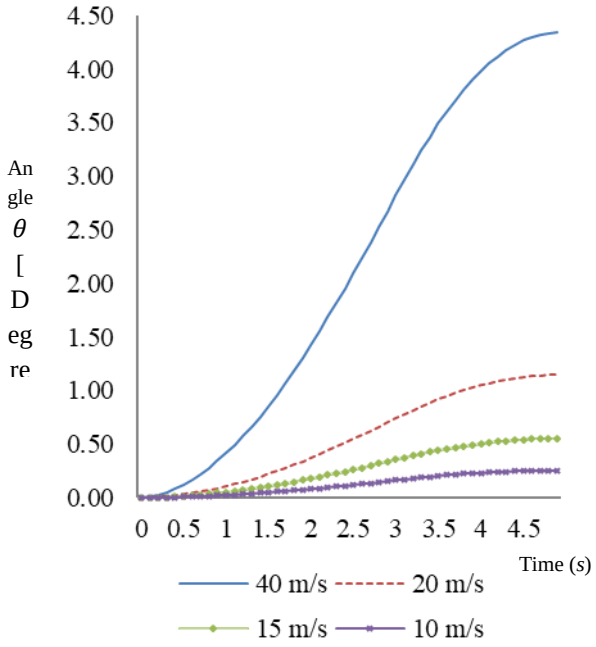

Fig.10: Time response of module when disturbed by wind velocities of 10, 15, 20 and 40m/s

Table 1 shows wind conditions of all four simulations, maximum angle θ, maximum drag force obtained by equation (2), drag force obtained by methodology proposed by international standard [18] and maximum module horizontal displacement:

Table 1: Maximum Drag Forces and Horizontal Displacement

v [m/s]	Max. θ [degrees]	F_D [kN]	F_D by API RP2A [kN]	Maximum horizontal displacement [m]
10	0,25	38,5	39	0,21
15	0,55	83,7	87,8	0,45
20	1,15	175	156,2	0,94
40	4,34	672,6	624,6	3,57

IV. CONCLUSIONS

It is observed that the maximum horizontal displacement values are consistent with field experience that large lifted bodies are subjected to pendulous displacement once disturbed by strong winds. Displacement amplitudes are large enough (0,94m) to hit nearby objects and people, as usually modules' lifting operations have small gaps to its landing targets and it is common practice to have operators nearby. It is also noted that such displacement occurs in a period of 4,5 seconds, which diminishes the ability to counter act and evacuate the affected area. Further, the simulated wind gusts have a duration of 3 seconds, if longer lasting gusts occur, there would be greater modules' displacement amplitude. Furthermore, at extreme wind conditions (40 m/s) such amplitudes can be greater than international standard [17] free space gap recommendation (3m). Although, at lower velocities, consistent with the ones experienced at Campos Basin, offshore Brazil, international standard 3-meter free space gap recommendation is sufficient to avoid collisions caused by wind induced displacement.

It is noted that aerodynamic forces applied to lifted body by wind conditions are great and it is also noted that the proposed methodology provides aerodynamic forces results in the same order of magnitude as the ones obtained applying API RP2A methodology.

Both observations lead to conclude that the proposed methodology is capable of estimating unwanted displacement caused by wind loads acting on lifted bodies. Further, it illustrates the importance of such evaluation prior to conducting a lifting operation to better manage the risks and avoid potential accidents as the displacement is significant and sudden.

REFERENCES

[1] U.S. Energy Information Administration (2016), Annual Energy Outlook 2016 with projections to 2040, U.S. Department of Energy, Washington, USA. Retrieved from https://www.eia.gov/outlooks/aeo/pdf /0383(2016).pdf

[2] Gerwick Jr., B. C. (2007), Construction of marine and offshore structures, 3rd ed., CRC Press.

[3] Nepal, B., Monplaisir, L., Singh, N.& Yaprak, A.(2008), "Product modularization considering cost and manufacturability of modules", International Journal of Industrial Engineering - Theory, Applications and Practice, 15(2), pp.132-142.

[4] Ross, B., McDonald, B.& Saraf, S. E. V. (2007), "Big blue goes down. The Miller Park crane accident", Engineering Failure Analysis, 14(6), pp.942 -961.

[5] Liu, Z., Wang, W., Zhang, A. (2013), "Construction Ventilation Scheme Optimization of Underground Main

https://dx.doi.org/10.22161/ijaers.611.57 *ISSN: 2349-6495(P) | 2456-1908(O)*

Powerhouse Based on CFD", Applied Mechanics and Materials, Vol. 368-370, pp.619-623.

[6] Silveira, B., Almeida, P. (2017), "Numerical Investigation of a Naca Air Intake for a Canard Type Aircraft",International Journal of Advanced Engineering Research and Science, Vol. 4, pp.032-040

[7] Zhao, K., Sakamoto, N., Koyamada, K., Tanaka, S., Murotani, K., Koshizuka, S. (2017), "Interactive visualization of large-scale 3D scattered data from a tsunami simulation", International Journal of Industrial Engineering: Therory, Applications and Practice, Vol.24, No. 2.

[8] Sharma, S., Raghav, V., Komerath, N., Smith, M. (2013), "Wall effect on fluid-structure interactions of a tethered bluff body", Physics Letters A, Vol.377, No.34-36, pp.2079-2082.

[9] Martins, D., Neto, A., Steffen, V. (2007), "A Pendulum-Based Model For Fluid Structure Interaction Analysis", Engenharia Térmica, retrieved from: http://servidor.demec.ufpr.br/reterm/ed_ant/12/artigo/ciencia/13_140.pdf

[10] White, F. (1991), Viscous Fluid Flow, 2nd ed., McGraw-Hill, New York.

[11] Monteiro, F. (2016), Análise da Influência de Cargas de Vento em Módulos Içados. Master's Thesis in Industrial Construction, Federal Fluminense University, Niterói, RJ.

[12] Menter, F. (1994), "Two-equation eddy-viscosity turbulence models for engineering applications", AIAA Journal, Vol. 32, pp.1598-1605.

[13] Versteeg, H., Malalasekera, W. (1995), An Introduction to Computational Fluid Dynamics - The Finite Volume Method, 1st ed., Longman Scientific & Technical, Essex.

[14] Filho, G., Silva, G., Segantine, E., Ribeiro, D., Romer, O. (2019), "A New Methodology to Analyze Fluid Pound in Sucker-Rod Pump Systems: Phenomenological Approach", International Journal of Advanced Engineering Research and Science, Vol. 6, pp.738-747.

[15] Sumer, M., Fredsoe, J. (2006), Hydrodynamics Around Cylindrical Structures: Advanced Series on Ocean Engineering – Volume 26, World Scientific Publ.Co, Denmark.

[16] Delaney, N., Sorensen, N. (1953), "Low-Speed Drag of Cylinders of Various Shapes", NASA Technical Reports Server, ID:19930083675, Retrieved from:https://ntrs.nasa.gov/search.jsp?R=19930083675

[17] Steggle, N. (1998), A Numerical Investigation of the Flow Around Rectangular Cylinders, Doctor of Philosophy Degree Thesis, The University of Surrey, Surrey.

[18] API RP2A (2010) – API Recommended Practice 2A. Planning, Designing and Constructing Fixed Offshore Platforms, The American Petroleum Institute, 22nd ed, US.